Check for updates

A fluorescent sensor array for rapid and facile point-of-care creatinine detection in saliva†

Rossella Santonocito, [iD] [a] Alessia Cavallaro, [iD] [a] Flavia Ficili,[a] Alessia Distefano,[a] Giuseppe Grasso,[a] Andrea Pappalardo, [iD] [ab] Nunzio Tuccitto [iD] *[a] and Giuseppe Trusso Sfrazzetto [iD] *[ab]

In recent years, the prevalence of kidney disorders has been increasing. In this context, creatinine is a crucial biomarker for assessing kidney function. Impaired kidney functions can lead to various acute and chronic conditions, including diabetic nephropathy, kidney cancer, abnormal glomerular filtration rate, and preeclampsia. Consequently, monitoring creatinine levels is essential for the prevention of serious kidney-related diseases and holds significant medical importance. In this study, we present a point-of-care device designed to detect creatinine levels in human saliva without pretreatment of a sample. This device is based on a sensor array containing different fluorescent chemical receptors (BODIPY, rhodamine, and naphthylamides) that interact with creatinine by non-covalent interactions, providing measurable changes in fluorescence output. To validate the device, calibration, recovery, and selectivity tests were performed. Notably, the array demonstrated a linear response to creatinine in a concentration range from 10 mM to 10 nM, as confirmed through partial least squares (PLS) analysis. Additionally, high selectivity was demonstrated by the excellent recovery of creatinine in an artificial saliva sample containing common interferents present in human saliva. Furthermore, our device was tested with real saliva, supporting the possibility to use this device in real life. This prototype represents the first point-of-care device able to quantify creatinine in human saliva in a single analysis, without pretreatments of the sample, covering a broader concentration range and a lower limit of detection (10 nM) with respect to other reported methods.

Introduction

Creatinine (Cre) is a by-product of muscle metabolism, routinely filtered and excreted by the kidneys. Creatinine plays a vital role as a biochemical marker for kidney function,[1] with abnormal concentrations indicating potential chronic kidney disease (CKD). However, the risk of kidney function interruption depends on the extent of abnormal concentrations of kidney biomarkers that ultimately act as a deciding factor for acute and chronic kidney disorders, diabetic nephropathy, kidney cancer, an improper glomerular filtration rate, and preeclampsia.[2]

Therefore, investigation of kidney biomarkers in various body fluids (such as urine, saliva, sweat, plasma, *etc.*) helps in diagnosis of kidney diseases/disorders to prevent huge problems related to the diseases, ensuring timely and effective treatment. Creatinine can be detected in a variety of biological fluids, including serum, saliva, urine, and blood. Table S1 (see ESI†) reports the standard and pathological creatinine concentrations in different biological fluids.[3] These ranges depend on gender and individual physiological factors, making precise and sensitive detection methods crucial for accurate diagnosis.[4] In clinical diagnosis, monitoring creatinine levels in the human body is crucial, as it serves as a key biomarker for physiological and pathological conditions. A decrease in creatinine levels below 40 μmol L^{-1} can indicate significant muscle mass loss, while levels reaching 500 μmol L^{-1} are associated with severe kidney disease (see Table S1, ESI†).[5]

Traditional detection techniques, such as the Jaffe method,[6] have historically been employed to measure creatinine levels. This method is based on the reaction between creatinine's methylene group and alkaline sodium picrate, resulting in the formation of a coloured compound. While widely used, the Jaffe method suffers from significant drawbacks, including interference from other molecules and low sensitivity, which can compromise accuracy in clinical applications.

[a] *Department of Chemical Sciences, University of Catania, Viale A. Doria 6, 95125 Catania, Italy. E-mail: giuseppe.trusso@unict.it*
[b] *INSTM Udr of Catania, Viale Andrea Doria 6, 95125 Catania, Italy*
† Electronic supplementary information (ESI) available: Characterization of probes, VIP analysis, setup of fiber, techniques used to detect creatinine in human matrixes, spectra obtained by fiber. See DOI: https://doi.org/10.1039/d5sd00063g

More advanced methods, such as ultra-high-performance liquid chromatography (UHPLC),[7] have been developed to address these limitations. UHPLC offers exceptional sensitivity and reliability but comes with challenges, including high costs, labour-intensive procedures, and the need for skilled operators and extensive sample pretreatment. Electrochemical techniques, based on enzymes selective for creatinine, represent another traditional approach.[8,9] These methods are portable and well-suited for point-of-care (POC) diagnostics, but they also face challenges related to enzyme immobilization, stability, and cost, limiting their widespread application.[10,11] To overcome the limitations of traditional methods, innovative detection strategies have emerged, such as molecularly imprinted polymers (MIPs)[12] and nanomaterials incorporating two-dimensional conductive materials.[13,14]

Another crucial point is the possibility to perform non-invasive diagnosis. In this context, saliva-based detection represents a particularly promising avenue. In fact, saliva sampling is easy, infection-free, and minimizes contamination risks, making it an attractive alternative to traditional blood and urine tests. Recent developments in screen-printed electrodes modified with nanozymes have enabled the creation of cost-effective and disposable diagnostic tools for saliva-based creatinine detection (Table 1).[15–17]

In this context, we have developed a portable optical array device capable of detecting creatinine in human saliva samples without pretreatments. Optical array sensors represent a class of sensing devices that simulate biological recognition mechanisms, in particular the human olfactory system for gas and the taste buds system for liquids: multiple receptors interact simultaneously with a complex mixture containing the target analytes.[17,18] In our case, the different receptors are fluorescent synthetic probes, each non-specific for the target analyte. However, after machine learning processing, the total responses, measured as changes in the fluorescence emission of each probe in the array, provide a distinctive fingerprint indicating the presence and concentration of creatinine. Selectivity and sensitivity are derived from the collective response of the probes, processed by machine learning and artificial intelligence (see Fig. 1).[19–24] Furthermore, by utilizing an optical fiber as a detector, we can measure the emission or colour change in both turn-on and turn-off responses.[25,26] Importantly, each
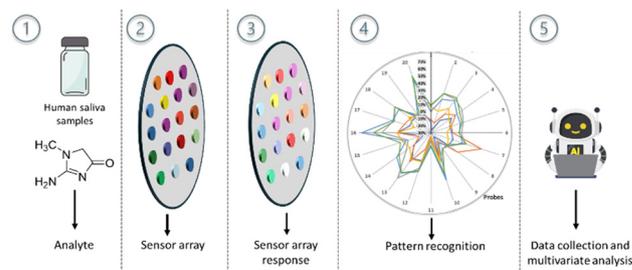

Fig. 1 Strategy proposed in this work: 1) collection of human saliva samples. 2) Fabrication of the sensor array. 3) Deposition of the analyte onto the array and collection of sensor array responses. 4) Data acquisition. 5) Data processing and multivariate analyses.

creatinine concentration generates a distinct radar plot shape, highlighting the potential for selective detection of creatinine.[27]

The target of our work is the detection of creatinine in the presence of the other interfering substances contained in human saliva with a single point-of-care (POC) device, containing 20 different synthetic fluorescent probes (see Chart 1). Compared to conventional analytical methods for creatinine detection, the use of synthetic receptors offers several advantages: (i) higher stability under a variety of analytical conditions, (ii) ability to detect creatinine together with structurally similar interfering substances without a false-positive response, (iii) direct analysis of real biological fluids without purifications or pre-treatments, and (iv) larger concentration range.

The interaction of each probe with creatinine was studied in the solid state using an optical fibre detector to monitor emission changes. The analysis was also conducted on artificial saliva and real saliva samples, demonstrating high selectivity and sensitivity without the need for pre-treatment. This is the first reported system able to detect creatinine, with a linear response in a concentration range from 10 mM to 10 nM, with such accuracy and selectivity in untreated biological fluids (saliva), using a single POC device.

Results and discussion

Design and synthesis

Chart 1 shows the chemical structures of the 20 fluorescent probes used in this work. The synthetic receptors used in our

Table 1 Techniques used to detect creatinine in human matrixes

Sensing material	Technique	Linear range	LOD mol L^{-1}	Human sample	Ref.
Working electrode modified	Non-enzymatic ECD	0.10 to 6.5 mmol L^{-1}	4.3×10^{-5}	Urine	12
Graphene nanoplatelet	MIB	1×10^{-1}–1×10^{9} pg ml^{-1}	1.7×10^{-13}	Human serum, urine	13
MIP based approach	Chip-sized MEMS-based	n.d.	8.8×10^{-7}	Serum	14
CuNPs	PSPCE	10 to 160 μM	1×10^{-7}	Blood and saliva	15
Nafion/polyacrylic gel Cu^{2+}/Cu$_2$O	CV/DPV	1–2000 μM	3×10^{-7}	Saliva	16

ECD = electrochemical determination; MIB = molecularly imprinted biosensor; MEMS = micro-electro-mechanical-systems; PSPCE = pretreated screen-printed carbon electrode; CV/DPV = cyclic voltammogram and differential pulse voltammogram; n.d. = not determined.
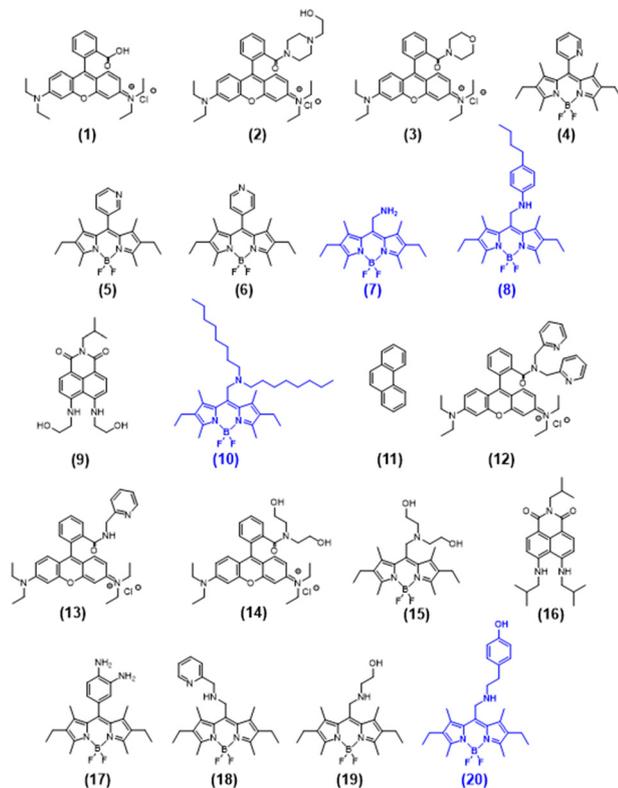
Chart 1 Chemical structures of the 20 fluorescent probes contained in the array sensor. New probes designed and synthetized in this work are reported in blue.

array are based on chromophores (rhodamine, BODIPY and naphthalimide scaffolds) able to cover a high emission range of fluorescence (from 400 to 700 nm).

These chromophores have been functionalised with functional groups able to interact with creatinine through single or multiple non-covalent interactions, such as hydrogen bonds, and dipolar and van der Waals interactions. Taking into account the chemical structure of creatinine, we designed new fluorescent probes ((7), (8), (10) and (20), Chart 1 in blue) with respect to the others yet synthetized in our laboratories (Chart 1, reported in black).[24] In particular, probes (8) and (10) should improve the creatinine sensing by van der Waals interactions due to the presence of aliphatic chains, while probes (7) and (20) should improve creatinine sensing by formation of hydrogen bonds due to the presence of amino and phenolic groups. In fact, as previously reported, supramolecular interactions with creatinine by hydrogen bonds can be involved using carboxylic acids,[28] or amide derivatives.[29] Synthetic pathways of these new probes are reported in Scheme S1 (see the ESI†).

Array preparation and calibration

A polyamide filter paper, activated with UV/O_3 treatment in order to remove any contamination and create active sites to facilitate interaction between the solid support and the probes, was used as a solid support for the array. Two

microliters of each probe (1 mM in chloroform) were dropped onto the solid support and the solvent was removed by evaporation at room temperature. Emission spectra of each probe were acquired with an optical fiber (λ_{exc} 366 nm) before (I_0) and after the addition of the creatinine solution (I_S), added by a common swab, and corrected by the contribution of pure water (I_W). In particular, the use of an optical fiber as a detector instead of a classical optical spectrometer reduces the cost and the size of the instrument. Our setup, as reported in Fig. S7 in the ESI,† is portable and compact, and can acquire high resolution emission spectra of each probe onto the solid support. It is ideal for practical applications because it does not require expertise of alignment, calibration and operation, in contrast to a classical spectrometer.[30,31]

All the data obtained at the maximum wavelength of the emission spectrum of each probe (mediated by three independent measurements) have been elaborated by multivariate analysis, obtaining the graphics reported in Fig. 2, which represents the array's response in terms of emission changes for each probe across varying creatinine concentrations, specifically ranging from 10 mM to 10 nM. In particular, the histogram in Fig. 2a reveals that each probe exhibits a unique emission response (in terms of turn-on or turn-off) across different creatinine concentrations.

Probes (7), (10), (13), (16), and (20) show the greatest enhancement, whereas probe (2) demonstrates the most significant quenching. This indicates that each probe is not
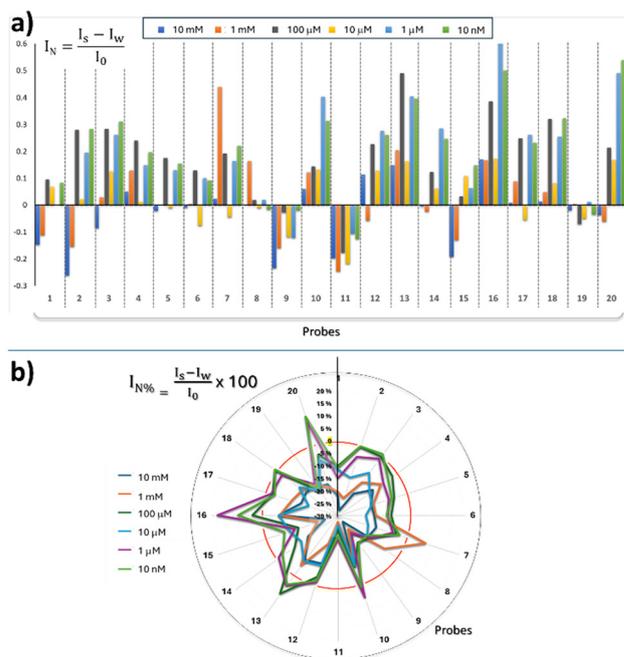

Fig. 2 a) Histogram plot showing the total response obtained in triplicate of the array after exposure to different concentrations of creatinine from 10 mM to 10 nM, using the formula ($I_N = [(I_S - I_W)/I_0]$). b) Radar plot showing the total response obtained in triplicate of the array after exposure to different concentrations of creatinine from 10 mM to 10 nM using the formula ($I_{N\%} = [(I_S - I_W)/I_0] \times 100$).

selective or specific for creatinine, but the combined response of all probes leads to a specific fingerprint, selective for each concentration of creatinine.

Meanwhile, the resulting intensity is determined using the equation ($I_{N\%} = [(I_S - I_W)/I_0] \times 100$), where I_S, I_W, and I_0 represent the sample intensity, the water intensity (used as a blank), and the initial intensity, respectively (each intensity value is derived from the average of three independent measurements). The radar plot in Fig. 2b is expressed as a percentage, with positive and negative values corresponding to increases (turn-on) and decreases (turn-off) in emission intensity, respectively. While turn-on sensors are generally preferred over turn-off sensors, the purpose of our array is to include multiple probes that respond differently, creating a unique analyte fingerprint.

Partial least squares (PLS) regression has been used to obtain a linear response of the array to the different creatinine concentrations. Fig. 3 shows the relationship between the expected (−log[M] scale) and predicted creatinine concentrations in the training set. This creatinine quantification plot is based on the average of three replicates and demonstrates a strong linear correlation between the predicted and experimental concentrations. Consequently, due to multivariate calibration, the array can detect creatinine at concentrations ranging from 10 mM to 10 nM. The method was validated by placing new array data in the PLS model, as shown in Fig. S8 (see the ESI†), showing that the data in red falls exactly on the calibration line.

Variable importance analysis (VIP), reported in Fig. S9 (see the ESI†), shows the importance of each probe in creatinine recognition. In particular, probes having a VIP value closed to 1 show the best and important response to creatinine. Notably, the new synthetized probes are in the best 4 positions.
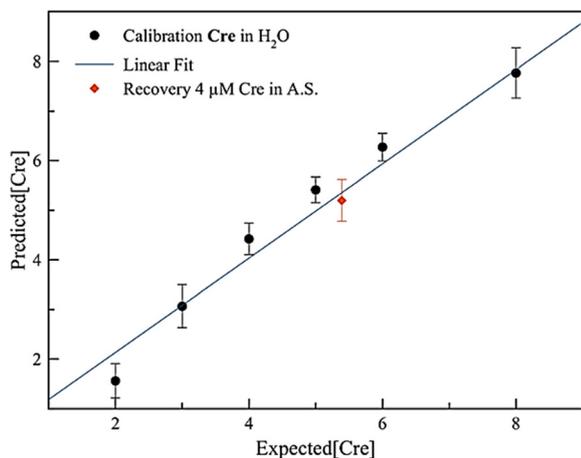

Fig. 3 Expected *vs.* predicted values of creatinine concentration expressed as (−log[M]) of 10 mM, 1 mM, 100 μM, 10 μM, 1 μM, and 10 nM calculated by the PLS model with 3 components. The red dot represents the addition of a known amount of creatinine (4 μM) in artificial saliva and the error bars in black represent the standard deviations calculated for the three replicates.

Validation: selectivity and recovery of creatinine

Additionally, to test the capability of this method to detect and quantify exact amounts of creatinine in a complex mixture, we prepared an artificial saliva sample having common analytes contained in real saliva.[32] In particular, we prepared artificial saliva (artificial saliva for pharmaceutical research, Sigma Aldrich) containing a known amount of creatinine (4 μM, such as the real concentration in saliva), in addition to the other common interfering substances: dopamine (0.1 nM); cortisol (3 nM); adrenaline (0.1 nM); noradrenaline (0.1 nM); glucose (2 nM); uric acid (200 μM); $NaNO_2$ (200 μM); urea (3.33 mM); KNO_3 (200 mM); KH_2PO_4 (2.42 mM).

The response of the array to artificial saliva was used to account for the contribution of all the interfering substances considered, with the aim of determining whether the array is still capable of providing a distinct fingerprint for creatinine, even in the presence of other analytes. Fig. 3 shows results in terms of recovery of the nominal creatinine concentration (4 μM) using the linear plot previously obtained. In particular, using the PLS model of the calibration of creatinine in water, we loaded the data obtained from the artificial saliva with creatinine standard addition as a secondary test dataset. As a result, we obtained a concentration of creatinine of 6.31 μM ($p[Crea]_{predicted} = 5.20$) very close to the real value of 4 μM ($p[Crea]_{expected} = 5.40$). As can be observed from the graphs in Fig. 3, the red dot represents the result obtained for creatinine. We can see that the red dot falls almost exactly at the point on the straight line corresponding to the nominal concentration of 4 μM, demonstrating the accuracy and the selectivity of the method, despite the presence of other common interfering substances in artificial saliva.

Determination of creatinine in human saliva sample

To evaluate the practical applicability of the developed biosensor in everyday life for medical application, the analysis of a real saliva sample was performed using the same materials and methodology described in the previous section. In this case, the device was exposed to untreated real saliva as well as to real saliva with standard additions of creatinine at concentrations of 4 μM [(−log[M]) = 5.4], 10 μM [(−log[M]) = 5], and 100 μM [(−log[M]) = 4]. The response of the array to saliva with standard additions can be compared to that of untreated saliva, and the results of the data analysis are presented in Fig. 4.

Given the absence of a standard protocol for analyzing creatinine in saliva, we have used the standard addition method. The PLS analysis reported in Fig. 4 shows that the calibration plot in an actual matrix obtained by the addition of 4 μM, 10 μM and 100 μM of creatinine, respectively, in real saliva showing a linear correlation between predicted and experimental values. In addition, to demonstrate that our array is able to quantify creatinine in real saliva, we analyzed the saliva sample without pre-treatment (*i.e.* centrifugation, or purification steps).
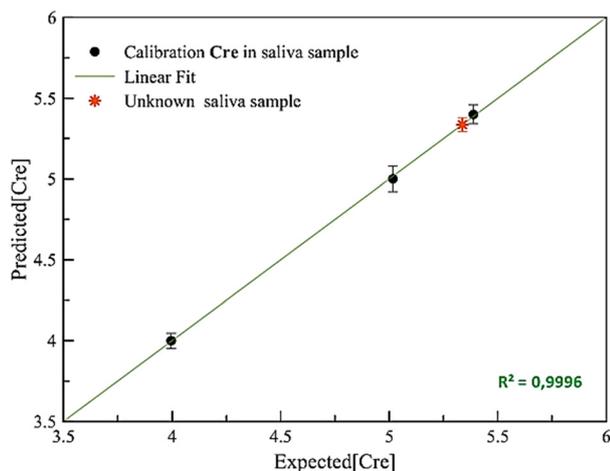
Fig. 4 Expected *vs.* predicted of creatinine concentration expressed as (−log[M]) of 4 μM, 10 μM and 100 μM in real saliva samples calculated by the PLS model with 3 components. The red dot represents the amount of creatinine calculated for the real saliva sample untreated. The error bars in black represent the standard deviations calculated for the three replicates.

We used the PLS model of the calibration creatinine in real saliva and we added as a secondary test set the data obtained from the array for real saliva. From the plot reported in Fig. 4, obtained through multivariate analysis, the concentration of creatinine calculated is 3.98 mM ($p[\text{Crea}]_{\text{real\_saliva}} = 5.34$).

Experimental

General experimental methods

Details of the synthetic procedures are reported in the ESI. The characterization of hyperspectral ultraviolet-induced visible fluorescence mapping (HUVFM) was conducted using a custom-built instrument. The analysis probe consists of a bundle of 19 Y-shaped fibers (BF19Y2HS02 sourced from Thorlabs), provided with a beam collimator (F220SMA-532 sourced from ThorLabs) separated by a watch glass from the analysis point. Among the 19 fibers, 10 are Y-ends connected to the source, which is a 365 nm LED sourced from Thorlabs. The remaining nine fibers are connected to an optical block housing a bandpass filter, which is designed to block backscattered light from the source. Subsequently, a CCD detector (CCS100/M sourced from Thorlabs) is connected to a bundle of optical fibers arranged linearly (BFL200HS02 sourced from Thorlabs), maximizing the light collected by the sampling led. Multivariate analysis of the dataset was performed by means of SIMCA-P9 (Umetrics). Dataset, was centred and unity scaled.

Sensing by array: calibration

Six solutions of creatinine at different concentrations (ranging from 10 mM to 10 nM) were prepared in MilliQ water (pH = 7). Three sensor arrays were exposed to each

solution, and the emission spectra were recorded before and after exposure, as detailed in the ESI.†

A blank measurement was also taken using MilliQ water. For statistical analysis, the following formula was applied: $(I_S - I_W)/I_0$, where I_S represents the emission of each probe after exposure to the analyte, I_W indicates the emission after exposure to MilliQ water, and I_0 corresponds to the emission before any exposure.

Fig. S10–S28 (see the ESI†) present the emission spectra of each probe (20 probes) in triplicate following exposure to the analyte (I_S) and the blank (I_W). However, Tables S2–S4 in the ESI† provide the complete spectral data for all tested concentrations.

Sensing by array: selectivity by recovery in artificial saliva sample

The recovery of creatinine in artificial saliva was assessed using three different solutions. To prepare the artificial saliva, dopamine (0.1 nM); cortisol (3 nM); adrenaline (0.1 nM); noradrenaline (0.1 nM); glucose (2 nM); uric acid (200 μM); $NaNO_2$ (200 μM); urea (3.33 mM); KNO_3 (200 mM); KH_2PO_4 (2.42 mM) were dissolved in artificial saliva (Artificial Saliva for Pharmaceutical Research, provided by Merck). For each solution, three sensor arrays were used, and fluorescence measurement was performed following the procedure described above for calibrations in water. A blank measurement was also taken using artificial saliva alone. For statistical analysis, the following formula was applied: $(I_S - I_{AS})/I_0$, where I_S represents the emission of each probe after exposure to the analyte, I_{AS} denotes the emission after exposure to artificial saliva, and I_0 corresponds to the emission before any exposure. Fig. S29–S47† show all the emission spectra of each probe (obtained in triplicate) and Tables S5 and S6† show the values taken at the wavelength maximum for each measurement.

Sensing by array: real samples

Saliva sampling from a human subject was carried out using Salivette®. Each Salivette® consists of a cotton swab, which the subject chewed for one minute. The swab was then wrung out through a sterile syringe into a vial for each subject and used without any pre-treatment. For creatinine detection, saliva samples were collected from one human subject and standard solutions of creatinine were added at concentrations ranging from 4 μM to 100 μM. As it was not possible to obtain a suitable blank measurement, the following formula was applied for statistical analysis: $(I_S - I_0)/I_0$, where I_S represents the emission of each probe after exposure to the analyte and I_0 corresponds to the emission before any exposure. Tables S7–S10 in the ESI† show the values taken at the wavelength maximum for each measurement in real saliva samples.

The saliva sample was collected from a healthy adult volunteer after obtaining written informed consent. According to the current regulations of the University of

Catania and Italian law (D.Lgs. 101/2018), the study did not require formal approval by the Ethics Committee, as it involved non-invasive collection from a single individual for methodological validation purposes.

Conclusions

In this study, a new optical method based on a fluorescent sensor array has been successfully employed for the fast and facile detection of creatinine in human saliva. The array comprises 20 selected probes, in particular four of these were synthetized *ad hoc* for the creatinine detection ((**7**), (**8**), (**10**), and (**20**)). All the probes were immobilised on a solid support and utilised in conjunction with an optical fibre system connected to a UV LED source and a detector. This setup enabled the detection and recording of emission spectra, facilitating solid-state creatinine sensing across a broad concentration range (10 mM to 10 nM).

Selectivity studies supported that the sensor array is able to detect creatinine even in the presence of common interfering substances in human saliva. In fact, our array has been tested with a real human saliva sample, detecting a creatinine concentration of 3.98 mM. These findings suggest that the developed sensing platform represents a promising approach for non-invasive creatinine monitoring.

Future work will focus on further validating the system through extensive testing on real biological samples, including saliva, urine, blood, and sweat. Additionally, optimisation of the sensor array's recovery and reusability will be explored to enable multiple analyses over time using the same device. These advancements will be crucial for the development of a robust, reproducible, and user-friendly diagnostic tool for clinical and biomedical applications.

This biosensor possesses key attributes such as high precision, a suitable linear calibration range and limit of detection and excellent stability, low cost, reliability, minimal sample quantity requirement, non-invasiveness, rapid response rate, and user-friendly operation.

Data availability

The data supporting this article have been included as part of the ESI.†

Author contributions

Conceptualization: N. Tuccitto and G. Trusso Sfrazzetto; investigation: R. Santonocito, A. Cavallaro, F. Ficili. G. Grasso, and A. Distefano. Validation: A. Pappalardo and N. Tuccitto; data curation: F. Ficili, A. Pappalardo, N. Tuccitto, G. Grasso, A. Distefano, and A. Cavallaro; writing – original draft: R. Santonocito and G. Trusso Sfrazzetto. Supervision: G. Trusso Sfrazzetto.

Conflicts of interest

There are no conflicts to declare.

Acknowledgements

Notes and references

1 S. Lopez-Giacoman and M. Madero, *World J. Nephrol.*, 2015, **4**, 57–73.

2 A. Jesuthasan, A. Ali, J. K. W. Lee and K. Rutherfurd-Markwick, *Nutrients*, 2022, **14**, 4685.

3 V. Mani, T. Beduk, W. Khushaim, A. E. Ceylan, S. Timur, O. S. Wolfbeis and K. N. Salama, *TrAC, Trends Anal. Chem.*, 2020, **135**, 116164.

4 E. Carias, H. Ferreira, T. Chuva, A. Paiva and J. Maximino, *World J. Oncol.*, 2022, **13**, 370–378.

5 R. B. Jadhav, T. Patil and A. P. Tiwari, *Appl. Surf. Sci. Adv.*, 2024, **19**, 100567.

6 E. P. Randviir, D. K. Kampouris and C. E. Banks, *Analyst*, 2013, **138**, 6565–6572.

7 A. Tkaczyk and P. Jedziniak, *Molecules*, 2020, **25**, 2445.

8 C. L. Gonzalez-Gallardo, N. Arjona, L. Alvarez-Contreras and M. Guerra-Balcazar, *RSC Adv.*, 2022, **12**, 30785–30802.

9 R. K. Rakesh Kumar, M. O. Shaikh, A. Kumar, C. H. Liu and C. H. Chuang, *ACS Appl. Nano Mater.*, 2023, **6**, 2083–2094.

10 C. S. Pundir, P. Kumar and R. Jaiwal, *Biosens. Bioelectron.*, 2019, **126**, 707–724.

11 M. K. Padwal, A. A. Momin, A. Diwan and V. Phade, *Indian J. Med. Biochem.*, 2023, **26**, 15–19.

12 S. N. Prabhu, C. P. Gooneratne and S. C. Mukhopadhyay, *IEEE Sens. J.*, 2021, **21**, 22170–22181.

13 Y. Li, L. Luo, M. Nie, A. Davenport, Y. Li, B. Li and K. L. Choy, *Biosens. Bioelectron.*, 2022, **216**, 114638.

14 C. L. Gonzalez-Gallardo, N. Arjona, L. Álvarez-Contreras and M. Guerra-Balcázar, *RSC Adv.*, 2022, **12**, 30785–30802.

15 T. M. F. do Prado, A. Garcia-Filho, T. A. Silva, F. H. Cincotto, F. C. de Moraes, R. C. Faria and O. Fatibello-Filho, *Talanta*, 2020, **207**, 120277.

16 A. Domínguez-Aragón, A. S. Conejo-Dávila, E. A. Zaragoza-Contreras and R. B. Dominguez, *Chemosensors*, 2023, **11**, 102.

17 S. Kalasin, P. Sangnuang, P. Khownarumit, I. M. Tang and W. Surareungchai, *ACS Biomater. Sci. Eng.*, 2020, **6**, 1247–1258.

18 Z. Li, J. R. Askim and K. S. Suslick, *Chem. Rev.*, 2019, **119**, 231–292.

19 Z. Li and K. S. Suslick, *Acc. Chem. Res.*, 2021, **54**, 950–960.

20 R. Santonocito, N. Tuccitto, V. Cantaro, A. B. Carbonaro, A. Pappalardo, V. Greco, V. Buccilli, P. Maida, D. Zavattaro, G.

Sfuncia, G. Nicotra, G. Maccarrone, A. Gulino, A. Giuffrida and G. Trusso Sfrazzetto, *ACS Omega*, 2022, **7**, 37122–37132.

21 R. Santonocito, R. Parlascino, A. Cavallaro, R. Puglisi, A. Pappalardo, F. Aloi, A. Licciardello, N. Tuccitto, S. O. Cacciola and G. Trusso Sfrazzetto, *Sens. Actuators, B*, 2023, **393**, 134305.

22 R. Santonocito, M. Spina, R. Puglisi, A. Pappalardo, N. Tuccitto and G. Trusso Sfrazzetto, *Chemosensors*, 2023, **11**, 503.

23 R. Santonocito, A. Cavallaro, R. Puglisi, A. Pappalardo, N. Tuccitto, M. Petroselli and G. Trusso Sfrazzetto, *Chem. – Eur. J.*, 2024, e202401201.

24 A. Cavallaro, R. Santonocito, R. Puglisi, A. Pappalardo, F. La Spada, R. Parlascino, M. Riolo, S. O. Cacciola, N. Tuccitto and G. Trusso Sfrazzetto, *Chem. Commun.*, 2024, **60**, 13702–13705.

25 R. Santonocito, A. Cavallaro, A. Pappalardo, R. Puglisi, A. Marano, M. Andolina, N. Tuccitto and G. Trusso Sfrazzetto, *Biosens. Bioelectron.*, 2025, **270**, 116986.

26 Y. Z. Fan, Q. Tang, S. G. Liu, Y. Z. Yang, Y. G. Ju, N. Xiao, H. Q. Luo and N. B. Li, *Appl. Surf. Sci.*, 2019, **492**, 550.

27 C. Liu, W. Zhang, Y. Zhao, C. Lin, K. Zhou, Y. Li and G. Li, *ACS Appl. Mater. Interfaces*, 2019, **11**, 21078–21085.

28 S. Goswami, S. Jana, A. Hazra, H.-K. Fun, S. Anjumc and A. Rahman, *CrystEngComm*, 2006, **8**, 712–718.

29 S. Jana, S. Prajapati, K. K. Suryavanshi, S. Goswami, R. Parida and S. Giri, *J. Phys. Org. Chem.*, 2020, **33**, e4066.

30 A. Leal-Junior, J. Silva, L. Macedo, A. Marchesi, S. Morau, J. Valentino, F. Valentim and M. Costa, *Sens. Diagn.*, 2024, **3**, 1135–1158.

31 G. Tunens, E. Einbergs, K. Laganovska, A. Zolotarjovs, K. Vilks, L. Skuja and K. Smits, *HardwareX*, 2024, **18**, e00530.

32 K. Ngamchuea, K. Chaisiwamongkhol, C. Batchelor-McAuley and R. G. Compton, *Analyst*, 2018, **143**, 81–99.